



EBPR process dynamics under variable conditions: interaction between PAOs and the microbial community

Valerie Liese^a, Berivan Akgün^b, Ahmed Elreedy^b, Jonas Lapp^b, Kilian Ferle^a, Raphael Moll^c, Johannes Gescher^b, Tobias Morck^{a,*}

^a Chair of Urban Water Engineering, University of Kassel, Kurt-Wolters-Straße 3, 34125 Kassel, Germany

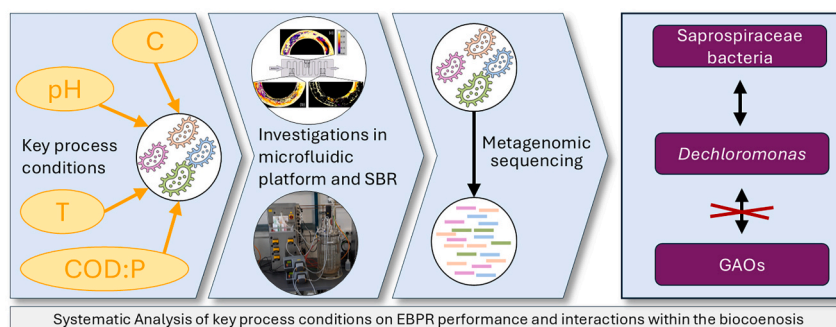
^b Institute for Technical Microbiology (TMI), Hamburg University of Technology (TUHH), Kasernenstraße 12, 21073 Hamburg, Germany

^c Department of Microbiology and Biotechnology, University of Hamburg, Ohnhorststraße 18, 22609 Hamburg, Germany

HIGHLIGHTS

- C-source type influences EBPR more than studied COD:P ratios, temperatures and pH.
- *Dechloromonas* plays a key role in EBPR, highlighting its prior underestimated role.
- PAO-GAO competition has no significant negative effects on EBPR performance.
- Microbial diversity contributes to a reliable phosphorus removal.

GRAPHICAL ABSTRACT



ARTICLE INFO

Keywords:

Enhanced biological phosphorus removal
Polyphosphate accumulating organisms
Microbial community
Biofilm system
Dechloromonas

ABSTRACT

The performance of enhanced biological phosphorus removal (EBPR) is influenced by various process conditions, such as the type of carbon source, temperature, COD:P ratio or pH-value. The activity of polyphosphate accumulating organisms (PAOs) and the composition of bioceonosis are strongly influenced by these process conditions. Nevertheless, critical knowledge gaps remain regarding the relevance of microbial diversity and the correlations between PAO/GAO community composition and EBPR process dynamics under different operational conditions. This study demonstrates that *Dechloromonas* plays a crucial role in the EBPR process and that the type of carbon source has a more sensitive influence on EBPR dynamics than the COD:P ratio, temperature or pH. Using both a microfluidic model biofilm system (MMBS) and a sequencing batch reactor (SBR) system, we found that the consumption of glucose resulted in maximal PAO activity, whereas EBPR performance was limited when using glycerol, ethanol and amino acids. In both systems, *Dechloromonas* was the dominant PAO, while in MMBS *Zoogloea* and in SBR *Competibacter/Contendobacter* were the dominant GAOs. *Tessaracoccus* (PAO) and *Micropruina* (GAO) were relevant in the fermentation of glucose and glycerol. No significant effect on EBPR performance was observed between 12 and 20 °C, and PAO activity peaked at pH 7.5. Our findings highlight that PAO-GAO competition is overestimated. We anticipate that our study provides a deeper understanding of the

* Corresponding author.

E-mail address: morck@uni-kassel.de (T. Morck).

dynamics in the biocoenosis and emphasizes the relevance of biodiversity in EBPR systems, which would help guide relevant applications.

Nomenclature

Parameter notation

BV	biofilm volume. mm^3/cm^2
DOC_{up}	dissolved organic carbon uptake. mgC/gVSS
κ_{rel}	phosphate release capacity. $\mu\text{gP}/\text{mm}^3$
κ_{rem}	phosphate removal capacity. $\mu\text{gP}/\text{mm}^3$
κ_{up}	phosphate uptake capacity. $\mu\text{gP}/\text{mm}^3$
η	phosphate removal efficiency. %
P_{rel}	phosphate release. μgP or mgP/gVSS
P_{rem}	phosphate removal. μgP
P_{up}	phosphate uptake. μgP or mgP/gVSS
$q_{\text{P,rel}}$	specific phosphate release rate. $\text{mgP}/(\text{gVSS}\cdot\text{h})$
$q_{\text{P,up}}$	specific phosphate uptake rate. $\text{mgP}/(\text{gVSS}\cdot\text{h})$

Abbreviation

C	carbon
Ac-Pr	acetate-propionate

BV	biofilm volume
C	carbon
COD	chemical oxygen demand
CLSM	confocal laser scanning microscope
DOC	dissolved organic carbon
EBPR	enhanced biological phosphorus removal
FISH	fluorescence in situ hybridization
GAO	glycogen accumulating organisms
MMBS	microfluidic model biofilm system
P	phosphate
PAO	polyphosphate accumulating organisms
PDMS	polydimethylsiloxane
PHA	polyhydroxyalkanoates
poly-P	polyphosphate
PCA	principal components analysis
SBR	sequencing batch reactor
VFA	volatile fatty acid

1. Introduction

Although the enhanced biological phosphorus removal (EBPR) process is inexpensive and environmentally sustainable (Liu et al., 2011a), its limitations and fluctuations in P-removal performance have led many operators of wastewater treatment plants (WWTPs) to continue prioritizing chemical phosphorus removal methods. Nevertheless, the EBPR process has received renewed attention as a research focus due to three relevant aspects: (i) EBPR is a key factor in making phosphorus recovery from wet sludge feasible, offering advantages over chemical precipitation by enabling improved phosphate (P) release associated with increased P availability (Egle et al., 2016); (ii) EBPR enhances the resilience of WWTPs to precipitant shortages, such as those temporarily experienced in Germany during the COVID pandemic, thereby reducing dependency on supply chain products (Eichholz et al., 2023); (iii) Due to distinct benefits, including superior settling properties, increased resilience to shock and toxic loads and improved dewaterability (Winkler et al., 2018), aerobic granular systems (AGS) are emerging as a relevant alternative to conventional sludge systems. The enrichment of polyphosphate-accumulating organisms (PAOs), which are responsible for EBPR, is essential for maintaining the long-term stability of aerobic granules (de Kreuk and van Loosdrecht, 2004).

In this context, many studies have yielded on identifying ecological niches and metabolic pathways of PAOs and the key factors influencing variations in EBPR performance, including wastewater temperature (Aghilinasrollahabadi et al., 2024; Liu et al., 2022; Lopez-Vazquez et al., 2007; Zheng et al., 2022), pH (Filipe et al., 2001; Nguyen et al., 2023; Oehmen et al., 2005), the availability and composition of carbon (C) sources (Shen and Zhou, 2016), and COD:P ratio (Broughton et al., 2008; Majed and Gu, 2020), among others. However, existing knowledge must be critically (re)examined and systematically evaluated for several compelling reasons.

First, many studies focus on systems with enriched PAO cultures under laboratory conditions, often investigating a single group of PAOs, such as *Accumulibacter* (Zheng et al., 2022) or *Tetrasphaera* (Liu et al., 2019; Nguyen et al., 2023).

While these studies provide valuable insights into the role of specific genera within the EBPR process, they represent only part of the broader

picture as recent studies have increasingly identified diverse genera of PAOs, prompting investigations into the specific ecological niches of individual microorganisms (Nielsen et al., 2019; Stockholm-Bjerregaard et al., 2017; Zhao et al., 2022). As a representative of the classic PAOs, *Accumulibacter* and *Dechloromonas* (currently designated as *Azo-nexus*; however, this paper adopts the commonly used former designation *Dechloromonas*) exhibit a metabolism in which volatile fatty acids (VFA) are assimilated and converted into polyhydroxyalkanoates (PHA) during the anaerobic phase, utilizing energy derived from polyphosphate (poly-P) hydrolysis and glycogen degradation. During the aerobic phase, PHA can be completely degraded to form poly-P, to regenerate the glycogen store and to impact biomass growth. With a markedly different metabolism, fermentative PAOs, such as *Tetrasphaera* and *Tessaracoccus*, assimilate amino acids, long-chain sugars and glucose, fermenting them into acetate. During fermentation, energy from poly-P hydrolysis is utilized to store glycogen. Typically, these fermentative PAOs are characterized by the absence of PHA storage; however, subspecies capable of storing PHAs have also been identified (Liu et al., 2019). Fundamentally, the poly-P hydrolysis induces the release of orthophosphate phosphorus ($\text{PO}_4\text{-P}$) back into the liquid phase, providing conclusions about the activity of PAOs (Dorofeev et al., 2020; Oehmen et al., 2007; Skennerton et al., 2015).

Second, the narrative that glycogen-accumulating organisms (GAOs) compete with PAOs, particularly for C-sources, has often led to process conditions being specified in the context of shifts in the relative abundances of GAOs and PAOs (e.g. Oehmen et al., 2005). Similar to PAOs, GAOs are adapted to alternating anaerobic and aerobic conditions, but do not contribute to phosphorus removal in EBPR systems. Instead, GAOs rely exclusively on glycogen degradation as an energy source to convert carbon substrates into PHA (Oehmen et al., 2007). Typical genera representing GAOs include *Micropruina*, *Deftuviicoccus*, *Competibacter*, *Contendobacter*, *Popionivibrio* (Nielsen et al., 2019). However, multiple studies have demonstrated that stable EBPR performance can be achieved even in the coexistence of PAOs and GAOs (Nielsen et al., 2019). Thus, it is still not clear to what extent PAOs and GAOs might interact or compete.

Third, as the overall performance of EBPR is determined by interactions within the microbial community, an increased emphasis on PAO and GAO biodiversity is crucial to understanding the EBPR process (Li et al., 2024). High-throughput gene sequencing technologies have

recently enhanced the ability to identify PAO and GAO taxa and are now becoming increasingly accessible. Consequently, several studies investigating the influence of boundary conditions on EBPR performance (e.g. Filipe et al., 2001; Guerrero et al., 2012; Puig et al., 2008) have not yet considered microbial biodiversity and the relevance of individual PAO and GAO genera in their systems, contributing to existing knowledge gaps regarding the correlations within the microbial community. Li et al. (2024) have attempted to address part of this knowledge gap by investigating microbial diversity in two EBPR systems. However, their study does not specifically examine the influence of different process conditions.

This is precisely the point at which our study contributes. We systematically investigated a range of process conditions, i.e., different types of C-source, COD:P ratios, temperatures, and pH values, while linking them to EBPR performance and, with particular emphasis, to their influence on PAO-GAO diversity, addressing the following two research questions: (i) How do specific process conditions affect EBPR performance dynamics and how is this correlated to the composition of the PAO-GAO community? (ii) Are specific key PAOs driving the EBPR process and how does microbial diversity contribute to maintaining reliable P-removal performance under varying conditions? To this end, a multivariate analysis was conducted on two different scales: a microfluidic model biofilm system (MMBS) and a sequencing batch reactor (SBR) system. These experiments were complemented by multiple analytical approaches, e.g., optical coherence tomography (OCT), which was applied in the MMBS, to elucidate the relationship between biofilm volume and phosphorus removal, whole native DNA sequencing to avoid amplification bias and thereby enabling an accurate assessment of the relevance of specific microorganisms, and principal component and network analyses to provide insights into correlations within the microbial community.

2. Materials and methods

2.1. Inoculation and growth conditions

Activated sludge from WWTP Langenhagen (Germany) served as inoculum (i.e., inoculum-LG) for MMBS and SBR. In addition, activated sludge from WWTP Ulm-Steinhäule (Germany) was inoculated (i.e., inoculum-US) into one of the SBRs to assess the impact of inoculum source on the process performance. Both WWTPs contain an anaerobic-anoxic-aerobic (A2O) process, characterized by a COD:P ratio ranging from 60 to 135, temperatures between 12.5 °C and 20 °C and pH values between 7.6 and 8.7. Denatured ethanol from brewery wastewater (12.5 % ethanol and 7.5 g/L acetic acid) is used as an external C-source in the WWTP Ulm-Steinhäule, while glycerol product (60 % glycerol, 5 % sodium and potassium) is utilized to enhance denitrification at the WWTP Langenhagen. For operation in the MMBS, the collected inoculum was initially sieved (160- μ m filters) prior to inoculation to remove large-size particles/granules. For the SBR system, no pre-treatment was necessary.

All experiments were conducted with a standard synthetic wastewater based on Smolders et al. (1994) as a cultivation medium to control the experimental conditions (composition is described in [supplementary information](#)). Unless otherwise mentioned, all experiments were performed using COD:P ratio of 40, and a mixture of sodium acetate and calcium propionate (at a COD-equivalent ratio of 75:25) or only sodium acetate as readily biodegradable C-sources. An overview of the standard operational conditions used in both systems is presented in the [supplementary information \(SI\)](#).

The varying key conditions selected for this study include the type of available C-source, temperature, COD:P ratio and pH. As C-sources, glucose, NZ-amine, pure ethanol, pure glycerol, denatured ethanol from WWTP Ulm-Steinhäule as well as the glycerol product from WWTP Langenhagen were used. While a wide range of C-sources were tested in the MMBS to gain a basic understanding of the EBPR process, the

investigation in the SBRs focused on glycerol and ethanol, as these C-sources are available and affordable on the market for wastewater treatment plant operators and thus may offer substantial practical benefits.

2.2. MMBS setup and operation

The microfluidic reactors, which have a polydimethylsiloxane (PDMS)-based meandering flow channel, were assembled according to Klein et al. (2022) (Fig. 1). The MMBS was continuously fed with two different media according to the desired growth cycle; the first, namely anaerobic medium, contains C-source (without P-source), while the second, namely aerobic medium, contains P-source (without C-source). The anaerobic and aerobic conditions were realized by purging the gasket around the microfluidic reactors with N₂ and compressed air, respectively, given the high gas-permeability of PDMS. Miniature active 2/2 valves were employed to implement alternating cycles of cultivation media and gases. The valves were controlled via a programmable custom-built unit. The gas flow rate was monitored by gas sensors (Honeywell, Airflow Sensor, 50CC/MIN, 25PSI, 5VDC). The flow-through MMBS was operated in 9-hour cycles consisting of anaerobic (3 h), interphase (1 h), aerobic (4 h) and interphase (1 h) stages. In the interphase, the aerobic medium (P without C-source) under N₂ atmosphere was supplied to provide the strict separation of the two main phases and to prevent carbon from being available to the microorganisms simultaneously with oxygen as an electron acceptor for their growth. The continuous media exchange and laminar flow effectively prevent the presence of nitrate in the anaerobic phase, thereby maintaining strictly anaerobic conditions. Due to the system's structure and scale, the sludge retention time (SRT) was not actively controlled and instead depended solely on the inconsistent washout of cells in the effluent.

Four series of experiments were performed independently considering: (I) acetate-propionate, pure ethanol, pure glycerol, glucose and NZ-amine as C-sources, (II) 12 °C as low-temperature conditions compared with ambient temperature (22–25 °C), (III) different COD:P ratios (100:10 = 10, 100:2.5 = 40 and 100:1.25 = 80), and (IV) different pH values of 6.5, 7.5 and 8.0 (experimental design is described in SI). Each experimental condition was tested in triplicate, with all replicates conducted in parallel (reported values represent means with standard deviations). To conduct the experiment at 12 °C, aluminium water-cooling blocks (40 × 120 × 12 mm) were used under the cultivation platform with a refrigerated circulation bath (VWR, 1160S, USA). The initial pH adjustment to the desired value was achieved using either 1 M-HCl or 1 M-NaOH. The acetate-propionate mixture was used as C-source in the temperature, COD:P and pH experiments. Each experiment commenced with an inoculation, followed by a 20-day cultivation period. At day 20 of each experiment, samples were taken every 30 min from the effluent over a complete anaerobic/aerobic cycle to quantify PO₄-P concentrations. The amounts of P-uptake and release were quantified considering the active P-release/uptake time (as illustrated in SI). Values recorded in abiotic control experiments were subtracted from the measured P-concentrations. P-release, uptake and biofilm removal capacities (indicated with the symbol κ) were estimated by dividing the relevant P-values (μ gP) by the corresponding volume of the formed biofilm (mm³).

2.3. SBR setup and operation

To facilitate the transfer from the biofilm to the activated sludge system, the process conditions established in the MMBS were adapted to a laboratory-scale SBR system (Sartorius B-DCU, Germany) comprising three automated reactors with an 8 L working volume each. Each reactor operated on an 8-hour cycle consisting of filling phase (10 min) including N₂-sparging, anaerobic phase (180 min), aerobic phase (240 min), settling (40 min) and decanting (10 min). With a volume exchange

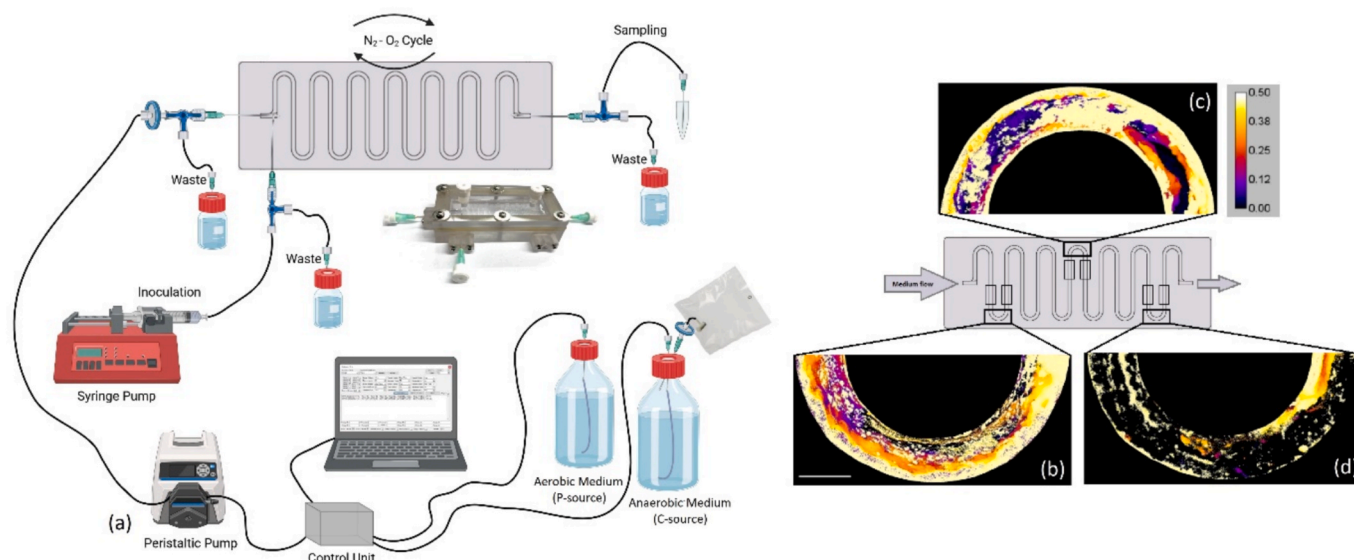


Fig. 1. The experimental setup for the cultivation of PAOs is shown schematically (a). Illustrative maps of mesoscopic biofilm structures in three sections of meandering channels are presented to depict biofilms' topography and local thickness: the front position (b), the middle position (c) and the back position (d). The scale on the right indicates the biofilm height in mm. Bar = 1 mm.

ratio of 25 %, 2 L were exchanged during the decanting and filling phase. To maintain volatile suspended solids (VSS) concentrations between 3.0 and 4.0 g/L (shown in SI), waste sludge was manually removed, thereby precluding control over a constant SRT. Continuous monitoring included real-time measurements of pH and redox potential, while temperature and dissolved oxygen (DO) concentration, set at 13 % saturation (approx. 1.2 mgO₂/L), were regulated at constant levels.

The analysis of process conditions was carried out over five adaptation phases between 2 and 5 weeks each. Following the initial inoculation with inoculum-US in SBR1 and inoculum-LG in SBR2 and SBR3, the adaptation phases proceed as follows: (I) acetate as reference (II) pure ethanol and pure glycerol, (III) denatured ethanol and the glycerol product as C-sources. After a second inoculation, subsequent adaptation phases included (IV) different temperatures (12 °C and 20 °C) and (V) different COD:P ratios (105:10.5 = 10, 420:42 = 10 and 420:5.25 = 80) (experimental design is described in SI). To capture stoichiometric and kinetic parameters, batch tests were conducted after each adaptation directly within the reactor. A well-defined starting point for the anaerobic kinetic evaluation was established by selectively dosing C- and P-sources immediately after completion of the filling phase with the synthetic medium. To exclude potential effects of denitrification on carbon consumption, nitrate concentrations were controlled at the onset of the anaerobic phase (corresponding values are provided in SI).

2.4. Analytical methods

To analyze the dissolved components, samples were first filtered using a pleated filter (2.0 µm), in case of sludge samples, followed by syringe filters (0.45 or 0.2 µm). Phosphate concentrations were determined using either Ion Chromatography (IC, Thermo Scientific Dionex IonPac AS9-HC) or molybdate spectrometric method (Cary 100 UV-Vis, Agilent, USA). DOC was measured by thermal-catalytic oxidation with NDIR detection (dimatoc 2000, Dimatec, Germany) and COD by a photometric cuvette system (DR 3900, Hach Lange). Standard methods were used for determining VSS and MLVSS. As part of the SBR sampling, a stoichiometric PHA-analysis was carried out for the beginning and end of anaerobic and aerobic phase to gain insights into the metabolic pathways. As preparation steps, sample duplicates were acidified with 98 % sulfuric acid and then washed three times, including the steps of centrifugation (4,500 g, 8 min, Multifuge X1-R, Fisher Scientific), withdrawal of supernatant, and re-suspension with ultrapure water.

After further centrifugation and decanting steps, the samples were stored at -18 °C. The actual PHA-determination, which includes the steps of freeze-drying, extraction, hydrolysis and esterification, phase separation and measurement via GC-FID (Agilent 8860 de-sign; Agilent Technologies™), was carried out according to (Laumeyer et al., 2023). PHA is described as the sum of PHB (Polyhydroxybutyrate) and PHV (Polyhydroxyvalerate).

2.5. Optical coherence tomography (OCT), fluorescence in situ hybridization (FISH) and confocal imaging

During cultivation in MMBS, mesoscopic structures of the mixture culture biofilms were observed via OCT technique, which allows an online investigation of biofilm structures under operational conditions. To estimate biofilm volume (BV), three positions were monitored, i.e., front, middle and back of the channel with two images of straight lines and one image of the corner for each position (Fig. 1), using a Ganymede™ spectral domain system (GAN200, Thorlabs GmbH, Dachau, Germany) with an LSM03 objective lens. Parameters were chosen as described earlier (Bauer et al., 2019) and digital images were analyzed with ImageJ/Fiji version 1.52p (Schindelin et al., 2012). Biofilm quantification was achieved using the relevant pixel signals with the voxel size derived from the imaging data (Klein et al., 2022). Biofilm height maps were also generated at the three positions, as illustrated in Fig. 1.

Fluorescence in situ hybridization (FISH) protocols, based on the fixation of cultured cells, were implemented as an endpoint analysis after 20 days of cultivation to verify results from metagenomic analysis. An automated FISH protocol was performed as described in Klein et al. (2024) with rRNA-targeted probes. Images of probe-labelled cells (shown in SI) were acquired using an LSM 800 confocal laser scanning microscope (CLSM) with a Plan-Apochromat 63x/1.40 Oil DIC M27 objective (Carl Zeiss, Oberkochen, Germany). Digital image analysis in microbial ecology (Daime) was used to quantify the abundance of microbial populations (Daims et al., 2006). For the FISH image analysis, the protocol was conducted as described in Daims (2009) to measure the biovolume fraction relative to the total biovolume of the entire detected microbial community. The percentage of *Dechloromonas* was determined using Daime version 2.2.

2.6. Metagenomic analysis, principal components analysis (PCA) and network analysis

For the metagenomic analysis, liquid samples were collected from the inocula LG and US and from the SBR at the end of adaption phase and stored at $-20\text{ }^{\circ}\text{C}$ until processing, while the biofilm from MMBS was flushed out after cultivation using minimal media and similarly stored at $-20\text{ }^{\circ}\text{C}$. The biomass was harvested by centrifugation at 13,000 g for 2 min. DNA was isolated using the Qiagen DNeasy PowerBiofilm kit (Qiagen, Hilden, Germany) following the manufacturer's instructions. The total concentration and purity of the extracted DNA were measured using a NanoDrop 2000 spectrophotometer (Thermo Scientific, Waltham, MA, USA) and the Qubit dsDNA assay kit (Life Technologies,

Carlsbad, CA, USA). For library preparation, 400 ng of Qubit double-stranded DNA per sample was used with the Native Barcoding Kit 24 V14, SQK-NBD114.24 (Oxford Nanopore Technologies, Oxford, UK). Sequencing was performed using a MinION Mk1b and an R10.4.1 flow cell with MinKNOW software v.24.02.6 (Oxford Nanopore Technologies, Oxford, UK). Basecalling and demultiplexing were executed using dorado v.7.3.9 in super accuracy mode. For taxonomic analysis and abundance estimation sequencing reads were aligned against MAGs of the MiDAS database (Singleton et al., 2021) using BLAST v2.12. Metagenomic bins were prepared for further characterization. Therefore sample-wise read assembly was conducted using Flye v.2.9.1-b1768 (Kolmogorov et al., 2020) with the additional parameters $-\text{nano-hq}$ and $-\text{meta}$. Minimap2 v.2.24 (Li, 2016) was used for read mapping.

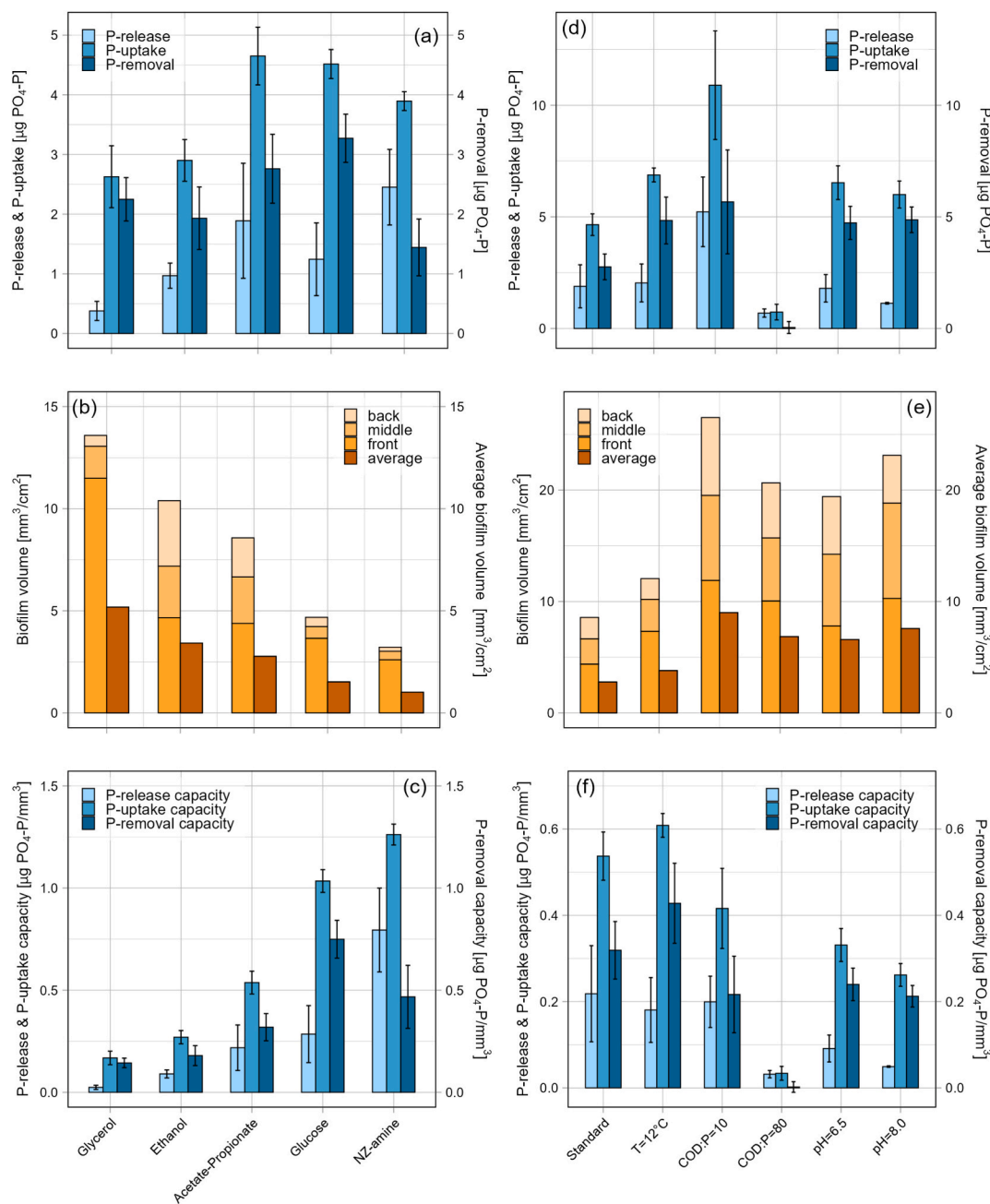


Fig. 2. (a,d) P-uptake, P-release and P-removal ($\mu\text{g PO}_4\text{-P}$), (b,e) biofilm volume and average biofilm volume (mm^3/cm^2) (corresponding standard deviation in SI), (c, f) biofilm P-uptake capacity, P-release capacity and P-removal capacity ($\mu\text{g PO}_4\text{-P}/\text{mm}^3$) for different C-sources or temperatures, COD:P ratios and pH values in the MMBS. Standard process conditions were conducted with acetate-propionate, room temperature, $\text{COD:P} = 40$, $\text{pH} = 7.5$. (The values represent the mean of triplicate measurements. Error bars indicate the standard deviation, with the corresponding numerical values provided in SI).

Contigs were annotated using Metabuli v1.9.0.2 (Kim and Steinegger, 2024) with the GTDB database r214 (Parks et al., 2022). The coverage of contigs was assessed using Minimap2 and Samtools 1.13. Binning was performed using taxvamb v4.1.4 (Kutuzova et al., 2024).

PCA was conducted, as a multivariate analysis tool, to study the variations among microbial communities and corresponding major performance indicators under the examined operational conditions, using Minitab 22.0. Further, spearman-based co-occurrence network analysis was conducted using R and Gephi 0.10; only significant

correlations ($p < 0.05$) were involved in the construction of the networks.

3. Results and discussion

3.1. Impact of carbon source composition on EBPR performance and PAO-GAO abundance

The results of P-release and P-uptake, shown in Fig. 2 and Fig. 3,

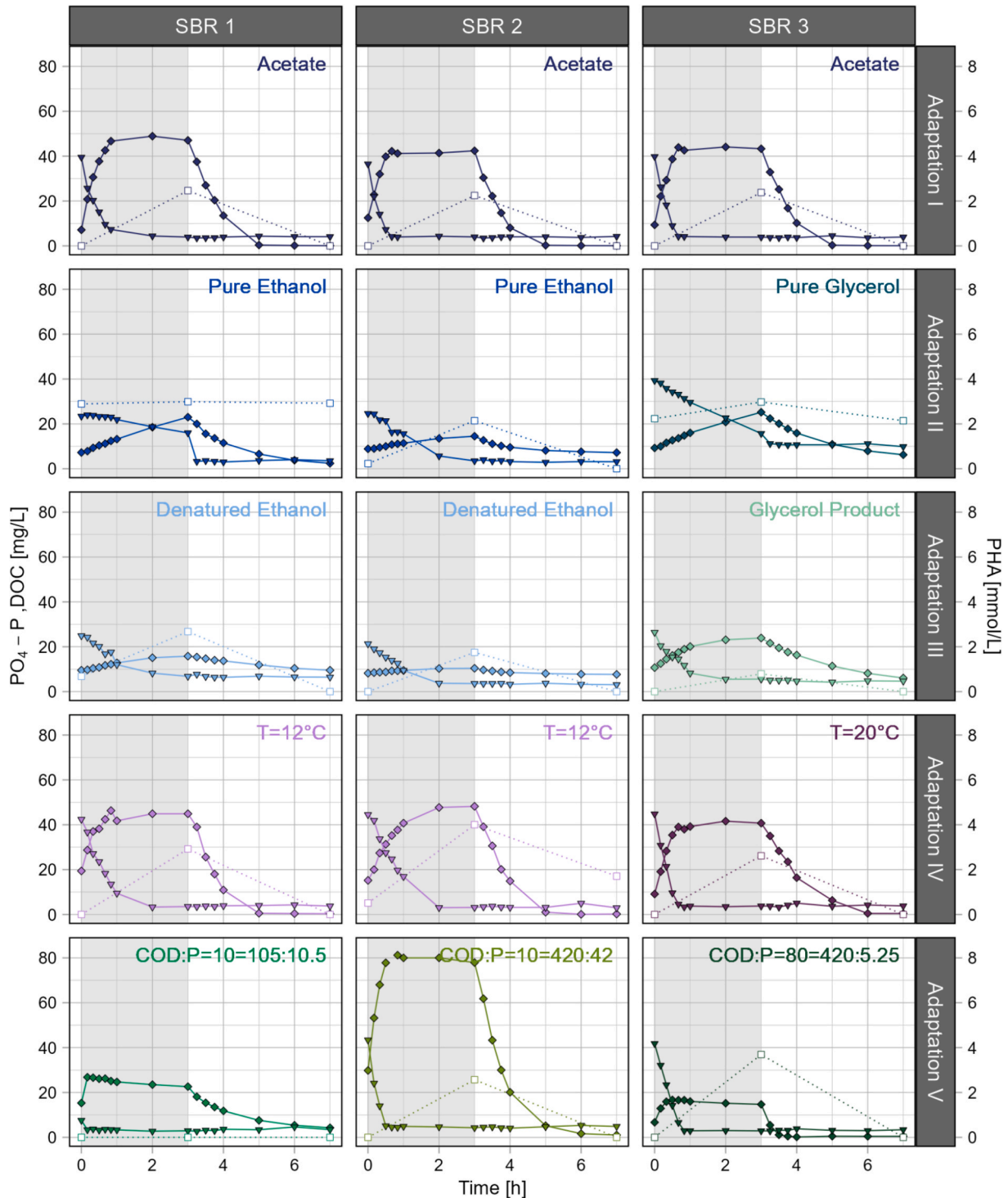


Fig. 3. PO_4 -P (◆), DOC (▼) profiles and PHA (□) values from the SBR batch tests for different C-sources, temperatures and COD:P ratios during anaerobic (grey background) and aerobic phase (white background). Standard process conditions were conducted with acetate-propionate, COD:P = 40 and $T = 20^\circ C$.

initially confirm the activity of PAOs across all tested C-sources. In the MMBS, a distinct influence of the C-source on biofilm growth is observed (Fig. 2b), with glycerol promoting to the highest biofilm volume ($BV = 5.18 \text{ mm}^3/\text{cm}^2$) and NZ-amine resulting in the lowest biofilm volume ($BV = 1.01 \text{ mm}^3/\text{cm}^2$). Fig. 2a clearly shows that increases in biofilm volume were accompanied by decreases in P-release, with NZ-amine showing the highest P-release ($P_{\text{rel}} = 2.45 \text{ } \mu\text{gP}$). NZ-amine also displayed the highest P-release capacity ($\kappa_{\text{rel}} = 0.79 \text{ } \mu\text{gP}/\text{mm}^3$) and P-uptake capacity ($\kappa_{\text{up}} = 1.26 \text{ } \mu\text{gP}/\text{mm}^3$). However, glucose achieved a significantly higher P-removal ($P_{\text{rem}} = 3.27 \text{ } \mu\text{gP}$) and P-removal capacity ($\kappa_{\text{rem}} = 0.75 \text{ } \mu\text{gP}/\text{mm}^3$). The P-removal capacity of glycerol ($\kappa_{\text{rem}} = 0.14 \text{ } \mu\text{gP}/\text{mm}^3$) and ethanol ($\kappa_{\text{rem}} = 0.18 \text{ } \mu\text{gP}/\text{mm}^3$) is considerably lower

compared to glucose ($\kappa_{\text{rem}} = 0.75 \text{ } \mu\text{gP}/\text{mm}^3$), NZ-amine ($\kappa_{\text{rem}} = 0.47 \text{ } \mu\text{gP}/\text{mm}^3$) and acetate-propionate ($\kappa_{\text{rem}} = 0.32 \text{ } \mu\text{gP}/\text{mm}^3$).

In the SBRs, the reference substrate acetate was observed to exhibit fast and extensive P-release, correlating with rapid carbon uptake (Fig. 3). Within less than 45 min, the DOC was depleted and a secondary P-release due to the anaerobic maintenance requirements of the biomass was observed to begin (Loosdrecht et al., 2016). Accordingly, an active PAO community was established in each SBR within the three-week adaptation I, achieving P-removal efficiency of up to 99 %. In contrast, a distinctly limited stoichiometric and kinetic P-release was observed in adaptation II and III. In SBR1 and SBR2 of adaptation II, the DOC was not completely taken up during the anaerobic phase and the

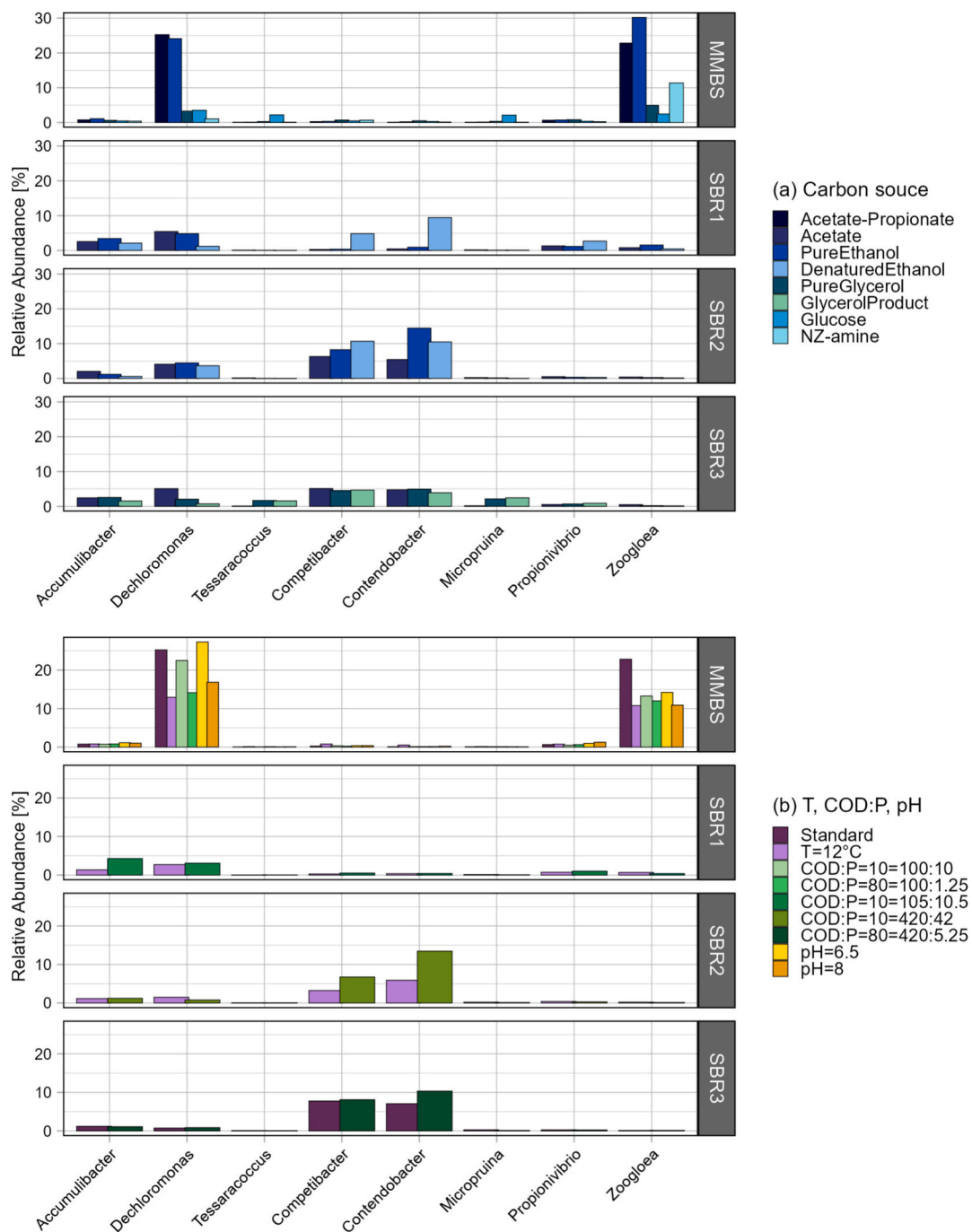


Fig. 4. Relative abundance of potential PAOs and GAOs comparing (a) different C-sources and (b) different temperatures, COD:P ratios and pH at the end of the cultivation in the MMBS and at the end of adaptations in SBR1–3. Abundance values are given in per cent of the total community. Standard process conditions in MMBS: COD:P = 40, T = Room temperature, pH = 7.5. Standard process conditions in SBR: COD:P = 40, T = 20 °C.

maximum P-release did not seem to be achieved within the three-hour phase, which prevented the determination of the secondary P-release rate. Therefore, only the total P-release was compared in the following analysis.

The findings revealed that P-release and P-removal efficiency depend on both the substrate and the inoculum. A comparison of pure ethanol between SBR1 and SBR2 indicates that specific P-release ($P_{rel,SBR1,II} = 5.57 \text{ mgP/gVSS}$, $P_{rel,SBR2,II} = 2.03 \text{ mgP/gVSS}$) and P-removal efficiency ($\eta_{SBR1,II} = 66.6 \%$, $\eta_{SBR2,II} = 18.7 \%$) are significantly higher for inoculum-US, whereas the specific DOC-uptake is only about one third as high (cf. SI). Also, inoculum-US demonstrates superior performance for denatured ethanol compared to inoculum-LG in terms of specific stoichiometric ($P_{rel,SBR1,III} = 5.57 \text{ mgP/gVSS}$, $P_{rel,SBR2,III} = 2.03 \text{ mgP/gVSS}$) and kinetic ($q_{P,rel,SBR1,III} = 2.40 \text{ mgP/(gVSS}\cdot\text{h)}$, $q_{P,rel,SBR2,III} = 0.66 \text{ mgP/(gVSS}\cdot\text{h)}$) P-release, however, this performance is reduced in both reactors compared to the use of pure ethanol, with minimal P-removal ($\eta_{SBR1,II} = 0.0 \%$, $\eta_{SBR2,II} = 6.6 \%$) occurring in both cases. A comparison of pure glycerol and the glycerol product indicates no significant differences. A significant difference, however, is that complete DOC degradation from the glycerol product is achieved within two hours, after which secondary P-release commences. In contrast, maximum P-release is not attained when pure glycerol is used.

The analysis of the PAO-GAO biocoenosis (Fig. 4a) reveals a substantial enrichment of *Dechloromonas* in the MMBS compared to the initial inoculum (cf. SI). The metagenome sequencing indicates that *Dechloromonas* exhibited the highest relative abundance (25.2 %) when acetate-propionate was supplied, closely followed by ethanol. In both cases, a co-enrichment of *Zoogloea* was observed, with ethanol appearing to promote its growth. Abundances of genus *Accumulibacter*, however, showed minimal enrichment at all MMBS experiments. In addition, under glucose supplementation, the relative abundance of *Tessaracoccus* and *Micropruina* approximately doubled compared to the inoculum. Although the enrichment of *Dechloromonas* was not as pronounced as in the MMBS, it prevails as the most abundant PAO in the SBR. The operation of SBRs were influenced not only by the process conditions but also by the inoculum used. In SBR1, microbial composition exhibits minimal variation between acetate and pure ethanol. However, upon the introduction of denatured alcohol, there was a marked enrichment of *Competibacter* and *Contendobacter*, accompanied by a significant depletion of *Dechloromonas*. Under same process conditions in SBR2, GAOs initially proliferate following acetate dosing and continue to accumulate in subsequent adaptations phases. Conversely, *Accumulibacter* showed a pronounced depletion indicating the decline in EBPR performance. Of note, the metagenomic sequencing results were corroborated by FISH via probing cells belonging to *Dechloromonas* (cf. SI); the proportion of *Dechloromonas* cells was then estimated (i.e., 28.0 %) using Daime analysis of FISH images.

The composition of PHA provides information about the dominant metabolism, which depends on the substrate but also on the microorganism. It is consistent with the current understanding that PHB accounts for the entire PHA-production when dosed with acetate (PHB:PHV ratio values in SI), as both PAOs and GAOs use acetate mainly for PHB-production and to a lesser extent for PHV-production (Oehmen et al., 2007). For ethanol or denatured alcohol, the results are inconsistent regarding the composition of PHA or the amount of formed PHA. In SBR2, only PHV is produced under both dosing conditions, whereas in SBR1, a proportion of PHB was also formed with the addition of denatured ethanol, comprising 29 % of the total PHA-formation. This indicates that a portion of PHA-production is likely attributable to the high abundance of *Contendobacter* and *Competibacter*. In contrast to PAOs, which are assumed to selectively produce PHA, these GAOs are thought to synthesize PHB and PHV randomly from acetyl-CoA and propionyl-CoA (Bengtsson, 2009; Oehmen et al., 2007). Another indication of GAO involvement in PHA production is the comparatively high quantity of synthesized PHA relative to the amount of phosphorus released in all three cases (PHA_{form}:P_{rel} ratio values in SI). In SBR3, a complete shift

from PHB to PHV occurred upon switching from acetate to glycerol. This is consistent with known microbial PHA pathways, where acetate preferentially feeds into acetyl-CoA, favoring PHB synthesis, whereas glycerol can be converted into propionyl-CoA, the key precursor for PHV formation (Elahinik et al., 2022). Consistently, *Dechloromonas*, commonly associated with acetate-based PHA accumulation (Liu et al., 2011a,b), declined in relative abundance, while increases in abundances of *Tessaracoccus* and *Micropruina* were observed (Fig. 4). Earlier genomic analysis showed that the abundant *Tessaracoccus* and *Micropruina* populations in glycerol-fed granules lack an identifiable PHA synthase (PhaC), while they possess glycerol uptake proteins and enzymes of the methylmalonyl-CoA/transcarboxylation route for propionyl-CoA (Elahinik et al., 2022; Gonzalez-Garcia et al., 2017). Meanwhile, this supports the hypothesis that they act as glycerol-fermenting fGAOs that produce propionate (a PHV precursor) rather than directly synthesizing PHV, which would explain the observed community-shift. This enrichment was less pronounced in the MMBS.

3.2. Impact of temperature, COD:P ratio and pH on EBPR performance and PAO-GAO abundance

The temperature experiments in the MMBS (Fig. 2) showed a slightly higher biofilm volume and P-removal at 12 °C ($BV = 3.79 \text{ mm}^3/\text{cm}^2$, $P_{rem} = 4.84 \text{ }\mu\text{gP}$) than at room temperature ($BV = 2.77 \text{ mm}^3/\text{cm}^2$, $P_{rem} = 2.76 \text{ }\mu\text{gP}$). In SBR2 and SBR3 (Fig. 3), a comparison between 12 °C and 20 °C reveals that the lower temperature has minimal effect on EBPR performance. The specific P-release ($P_{rel,SBR2,IV} = 12.1 \text{ mgP/gVSS}$, $P_{rel,SBR3,V} = 12.7 \text{ mgP/gVSS}$), DOC-uptake ($DOC_{up,SBR2,IV} = 15.2 \text{ mgC/gVSS}$, $DOC_{up,SBR3,IV} = 16.1 \text{ mgC/gVSS}$) and P-removal efficiencies ($\eta_{SBR2,IV} = 98.7 \%$, $\eta_{SBR3,IV} = 95.2 \%$) observed in both reactors are comparable. While P-release occurs notably faster at higher temperatures ($q_{P,rel,SBR2,IV} = 9.4 \text{ mgP/(gVSS}\cdot\text{h)}$, $q_{P,rel,SBR3,IV} = 17.8 \text{ mgP/(gVSS}\cdot\text{h)}$), uptake is even slightly accelerated at lower temperatures ($q_{P,up,SBR2,IV} = 12.5 \text{ mgP/(gVSS}\cdot\text{h)}$, $q_{P,up,SBR3,IV} = 9.4 \text{ mgP/(gVSS}\cdot\text{h)}$). According to Erdal et al. (2008), at low temperatures, glycogen metabolism was diminished, thereby allocating more energy toward PHA synthesis and phosphorus uptake. PAOs typically utilize the Embden–Meyerhof–Parnas (EMP) pathway for glycogen degradation, with *pfkA* serving as a key enzyme for the EMP pathway. The activity of *pfkA* is strongly influenced by temperature, which thereby acts as a regulator in controlling glycolytic pathway utilization (Erdal et al., 2008; Tian et al., 2025). Tian et al. (2025) reported a marked reduction in *pfkA* gene expression at 12 °C, indicating that low temperature slows glycogen metabolism from the perspective of gene expression. In SBR1, P-release ($P_{rel,SBR1,IV} = 8.7 \text{ mgP/gVSS}$) is noticeably constrained compared to SBR3 and to SBR1 (adaptation-I) under 20 °C. However, a relatively high initial phosphorus concentration was observed as a starting value in the batch test (Fig. 3), which may contribute to potentially inconsistent interpretations. Furthermore, PAOs are dominant in SBR1, whereas GAOs prevail in SBR2 and SBR3, reflected by variations in the relative abundances of *Competibacter* and *Contendobacter*. These patterns are likely associated with the distinct inocula and driven by subgenus-level differences in gene expression and metabolic responses, which could not be sufficiently resolved with the data present.

In the MMBS, higher P-concentrations of 10 mgP/L (COD:P = 10) under conditions of sufficient carbon availability (Fig. 2) resulted in enhanced biofilm growth ($BV = 8.99 \text{ mm}^3/\text{cm}^2$) and increased P-release ($P_{rel} = 5.67 \text{ }\mu\text{gP}$) compared to COD:P = 40, due to higher P-availability. This is further corroborated by the high P-release and P-removal efficiency in SBR2 ($P_{rel,SBR2,V} = 16.6 \text{ mgP/gVSS}$, $\eta_{SBR3,V} = 96.5 \%$). Low P-concentrations (COD:P = 80) resulted in reduced poly-P formation during the aerobic phase, thereby limiting the P-release in the anaerobic phase. This is evident in both the MMBS ($\kappa_{rel} = 0.03 \text{ }\mu\text{gP}/\text{mm}^3$) and the SBR3 ($P_{rel,SBR3,V} = 3.9 \text{ mgP/gVSS}$). While P-removal capacity in the MMBS was negligible, a P-removal efficiency of 93.1 % is achieved in SBR3. Low COD concentrations (COD:P = 10), as applied in SBR1, lead

to reduced PHA-formation by PAOs during the anaerobic phase, resulting in a lack of energy for poly-P formation during the aerobic phase. This assumption is confirmed by the absence of measurable PHA (Fig. 3) and a significantly lower P-removal efficiency ($\eta_{\text{SBR1,V}} = 72.1\%$), compared to SBR2 ($\eta_{\text{SBR1,V}} = 96.5\%$) and SBR3 ($\eta_{\text{SBR1,V}} = 93.1\%$).

The investigation of COD:P ratio revealed no direct correlation between COD:P ratio itself and P-release and P-removal efficiency. Instead, our results suggest that the absolute nutrient concentrations exert a decisive influence. This is evidenced by the reduced P-release and P-removal performance under carbon limitation in SBR1 (COD:P = 10, $P_{\text{rel,SBR2,V}} = 5.56 \text{ mgP/gVSS}$, $\eta_{\text{SBR1,V}} = 72.1\%$) and under phosphorus limitation in SBR3 (COD:P = 80, $P_{\text{rel,SBR3,V}} = 3.90 \text{ mgP/gVSS}$, $\eta_{\text{SBR3,V}} = 93.1\%$), when compared to SBR2 (COD:P = 10, $P_{\text{rel,SBR2,V}} = 16.6 \text{ mgP/gVSS}$, $\eta_{\text{SBR3,V}} = 96.5\%$), which exhibited increased P concentrations. Additionally, in the SBR2, PAOs were present in only low abundance despite the high P-release, while the relative abundance of *Competibacter* and *Contendobacter* increased significantly (Fig. 4b). In contrast, GAOs exhibited minimal relative abundance in SBR1, despite the same COD:P ratio. Overall, the COD:P ratio must be considered in conjunction with the total concentration of C and P, as both have a limiting effect. This investigation and the study of Majed and Gu (2020) demonstrate that PAOs perform well at low COD:P ratios of 10, as long as sufficient P is available. This highlights the advantage of the energy derived from poly-P hydrolysis compared to GAO, which provides a competitive advantage for PAOs over GAOs (Oehmen et al., 2007).

Regarding the effect of pH on MMBS performance, the behaviour of P-releases during the anaerobic phase remained relatively consistent between pH 6.5 and 8.0. This is likely attributed to the lower sensitivity of substrate uptake, PHA production, and glycogen consumption to pH changes under anaerobic conditions, as discussed earlier by Nguyen et al. (2023) and Wang et al. (2013). Meanwhile, the observed variation in P-uptakes during the subsequent aerobic phase in this study can be attributed to the hypothesis that PHA consumption, phosphate uptake rates and biomass growth by PAOs are sensitive to changes in pH levels (Filipe et al., 2001; Liu et al., 2007). Higher relative abundances of *Dechloromonas* were observed at pH 6.5 and 7.5 compared with pH 8.0 (Fig. 4b), which is consistent with former physiological and P-removal studies to report $\text{pH} \leq 7.5$ as optimal for *Dechloromonas* species (Horn et al., 2005; Kang et al., 2019).

3.3. Relevance of specific PAO and GAO genera

In both the MMBS and SBRs, although certain potential GAOs and PAOs and their correlations were identified, only selective genera of PAOs and GAOs appeared to be significant in term of their abundance. *Dechloromonas* emerged as the most abundant PAO, dominating both systems. This organism seems to have a growth advantage over *Accumulibacter*, which, while also significantly present, exhibited lower abundance, as well as over the low-abundance *Tessaracoccus*. In MMBS, a particularly strong accumulation of *Dechloromonas* up to 25 % relative abundance was observed under acetate-propionate and ethanol feeding conditions. *Tessaracoccus* appears to play a role as a fermentative PAO, as evidenced by its enrichment with glucose in the MMBS and glycerol in the SBR. Guerrero et al. (2012) and Nielsen et al. (2019) suggested that the 16S rRNA amplicon sequencing method overestimates the abundance of *Dechloromonas* and *Tessaracoccus*, implying that its relevance to the EBPR process may be overestimated. However, this study used whole-genome sequencing to avoid amplification bias. Consequently, the relevance of *Dechloromonas* and *Tessaracoccus* has previously been likely underestimated.

Regarding the abundance of GAOs, a clear distinction can be observed between the MMBS and the SBR. In the MMBS, *Zoogloea* is highly abundant, whereas in the SBR, *Competibacter* and *Contendobacter* are more prominent. A potential explanation for such variation is the difference in reactor cultivation conditions. In MMBS, a microfluidic cultivation reactor with meandering microchannels with 150 μL

working volume and very high surface area-to-volume ratio of $\sim 5,900 \text{ m}^2/\text{m}^3$, which greatly facilitates efficient attachment and biofilm formation. Additionally, fluid shear forces in the flow-through system stimulate biofilm formation by enhancing EPS production and promoting the availability of nutrients necessary for microbial growth (Zheng et al., 2021). This is considered as favorable conditions for *Zoogloea*, which was well-reported as excellent candidate for EPS biosynthesis and floc formation (Wang et al., 2024), resulting in the selective proliferation on carrier material, which was not the case in the SBRs as suspended growth systems.

An additional specific view on individual process conditions reveals that the highest P-removal was achieved when glucose was used as C-source. Here, *Tessaracoccus* and *Micropruina*, both known for their fermentative metabolism, appear to play a role in EBPR performance, as their abundance increased under glucose dosing. The products of glucose fermentation are likely to be made available to *Dechloromonas* and *Zoogloea*. When dosing glycerol and ethanol, both systems consistently exhibit significantly lower P-release/uptake performance compared to acetate or acetate-propionate. The stoichiometric results from the MMBS and SBR, as well as the kinetic values from the SBR, are consistent with the findings of Guerrero et al. (2012), which suggest that glycerol is a suitable additive, provided that a sufficient anaerobic hydraulic retention time (HRT) is maintained. This statement can also be extended to ethanol, in agreement with the studies of Puig et al. (2008), as well as to denatured ethanol and the glycerol products. On another hand, despite its low abundance, the relevance of *Micropruina* as a fermenting GAO becomes apparent under conditions involving the dosing of glucose and glycerol. Regarding the presence of genus *Propionivibrio* in both systems, its low abundance, however, renders it largely irrelevant to this investigation.

Moreover, Lopez-Vazquez et al. (2009) reported that PAOs dominate over GAOs under acetate-propionate dosing at temperatures of 10 °C, a finding consistent with results of SBR1 in this study. However, *Competibacter* and *Contendobacter* were dominant over PAOs in SBR2 and SBR3. Consequently, this study does not support the conclusion of Lopez-Vazquez et al. (2009) that the inhibition of GAOs explains the stable performance of EBPR at low temperatures. Instead, our findings indicate that temperature exerts only a minor effect on PAO activity and EBPR removal performance. In the MMBS, *Dechloromonas* was significantly dominant over *Zoogloea*. While our study focuses on changes in relative abundance and does not directly investigate metabolic regulation of PAO lineages, the observed shifts in *Dechloromonas* and other key PAOs and GAOs provide an initial indication of community dynamics under different conditions. Future work incorporating pangenomic or metatranscriptomic analyses could reveal clade-level functional differentiation and metabolic regulation within these lineages.

3.4. Correlations between PAO/GAO abundances and EBPR process dynamics at different process conditions

To visualize and analyze the distribution of PAOs/GAOs under various operational conditions and explore potential correlations with biofilm formation/activity, a PCA was conducted. For MMBS, this analysis was based on the relative abundance of major PAOs/GAOs, biofilm volume, P-release, P-removal and biofilm P-removal capacity. The results show that PC1 and PC2 together explain 65.9 % of the total variance, indicating that variations are acceptably defined by the available samples (Fig. 5). For SBR, PCA was conducted using the relative abundance of potential PAOs/GAOs in combination with the corresponding specific P-uptake/release and P-removal efficiency under different conditions. The results showed a total variance of 61.6 % for PC1 and PC2.

The score plot (Fig. 5a) reveals that MMBSs fed with acetate-propionate exhibited behaviour with noticeable variations at different temperatures, COD:P or pH compared with the effect of other C-sources. The use of other C-source compositions induced larger variations for

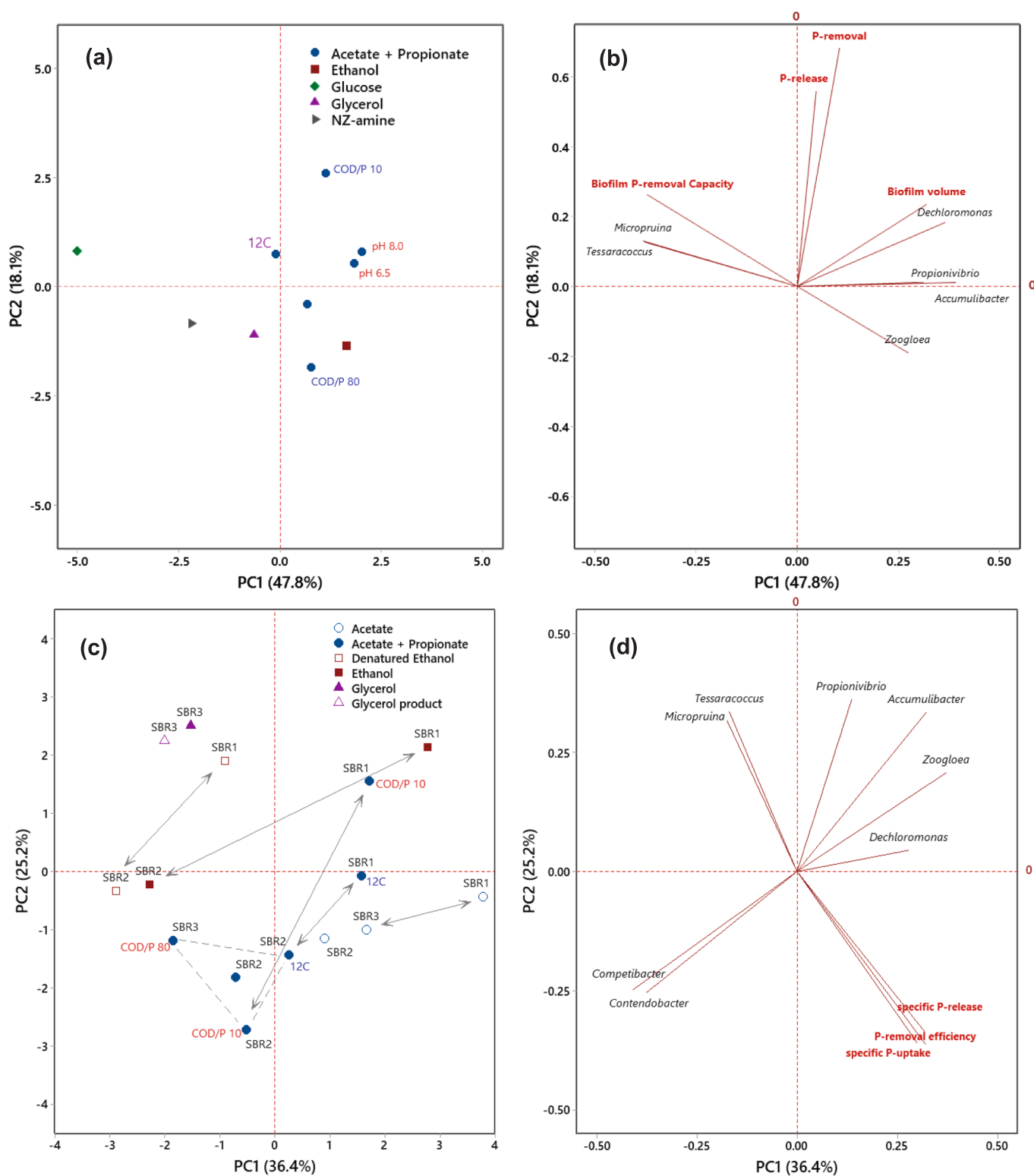


Fig. 5. (a, b) Score and loading plots derived by PCA based on relative abundance of major PAOs and GAOs in MMBS operated at different C-sources, temperature, pH, and COD:P, as well as corresponding biofilm volume and P-release, P-removal and P-removal capacity. (c, d) Score and loading plots derived by PCA based on relative abundance of major PAOs and GAOs in SBRs operated at different C-sources, temperature and COD:P, as well as corresponding specific P-uptake/release and P-removal efficiency. PC implies the principal component; arrows, in the score plots, are used to highlight the variance between samples.

glucose and NZ-amine, excluding ethanol and glycerol which resulted in minimal variation. The loading plot (Fig. 5b) shows that biofilm volume was negatively correlated with its P-removal capacity, which is likely due to substrate/nutrient diffusion limitations and the resulting growth of competing bacteria. P-release and P-removal exhibited a strong positive correlation, suggesting that P-removal is primarily driven by P release or PAO activity rather than by P-incorporation through biomass growth within the biofilm. The dominant genera *Dechloromonas* and *Zoogloea* were positively correlated; the well-known PAOs *Dechloromonas* and *Accumulibacter* were positively correlated with biofilm formation. Given the high abundance of *Zoogloea* and the shown weak correlation with performance indicators, its potential activity as PAOs seems unsupported. This aligns with the reported presence of *Zoogloea* in biofilms, regardless of P-removal efficiency (Sandeep et al., 2023). Other potential GAOs, such as *Micropruina*, showed negative correlations with the dominant *Dechloromonas* and *Zoogloea*.

For the SBRs, the score plot (Fig. 5c) reveals that feeding with acetate-propionate exhibited behaviour with minimal variation, regardless of the applied COD:P ratios and temperatures, compared to those fed with other C-sources. Glycerol and ethanol exhibited larger variations with acetate or acetate-propionate, in the system than those observed in the MMBS. Moreover, the use of different inoculum origin (i. e., inoculum-US in SBR1) showed substantial variation (highlighted by the arrows in Fig. 5c), under all tested conditions, when compared with SBR2 or SBR3, which were inoculated from same origin. These differences point to distinct gene expression patterns and metabolic responses at the subgenus level within the PAO and GAO clades (Li et al., 2024), aspects that were not examined in detail here. The loading plot (Fig. 5d) shows strong positive correlations between the major performance indicators under different conditions, indicating dominant P-removal activities. Meanwhile, no strong correlations were observed between the abundant genera *Contendobacter* and *Competibacter* and the used performance indicators, which might support their potential role as GAOs. Similarly, the less abundant *Zoogloea* showed no clear correlation with performance indicators, aligning with its position in the MMBS samples. This contrasts with *Dechloromonas*, which showed a positive correlation with performance indicators, emphasizing its role in P-removal under varying operational conditions. A comparison of the intercorrelations between major PAOs/GAOs in the MMBS and SBR revealed similar trends, such as the negative correlation between *Dechloromonas*, *Zoogloea*, and *Accumulibacter* versus *Contendobacter* and *Competibacter*, as well as between *Dechloromonas* and performance indicators. In addition, the aforementioned hypothesized role of *Micropruina* and *Tessaracoccus* in fermenting glycerol in the SBR can be further shown by the strong positive correlation shown by the score plot as well as the direction of their vectors in the loading plot towards glycerol samples (Fig. 5c).

3.5. Correlations among PAOs and GAOs in the biocoenosis before/after enrichment

Spearman-based co-occurrence networks (corresponding figures in SI) were conducted for genera (with an abundance of > 1 %) in samples taken before and after enrichment under different conditions, to examine overall distribution and potential clusters.

For MMBS, spearman-based co-occurrence network, including samples before enrichment, shows four modularity clusters, where *Dechloromonas* and *Zoogloea* (as potential PAOs/GAOs) grouped in one cluster. This cluster (light-blue coloured) had mainly negative correlations with other clusters (either those contain dominant genera in inoculum samples or major GAOs), highlighting the enrichment efficiency under the employed P-accumulation conditions; further, neither *Contendobacter* nor *Competibacter* genera were found in this cluster, emphasizing their minor role within the enriched microbial community. When inoculum samples were excluded from the construction of network and nodes (representing genera) were ranked based on their

betweenness centrality, it was noted that *Dechloromonas* had a high betweenness centrality rank, suggesting a more central structural position relative to other genera (c.f. SI for spearman-based co-occurrence network, excluding samples before enrichment). Most of its significant correlations were found as negative with other genera, emphasizing on being a key player in the observed P-removal performance under different conditions. This was not the case for *Zoogloea*, which had a lower rank with only one positive significant correlation with *Dechloromonas*. An et al. (2016) reported that *Dechloromonas* and *Zoogloea* possess EPS biosynthesis gene cluster(s), which facilitate their selective proliferation within the system and contribute to biofilm development and stability. Due to sufficient EPS formation capacities, *Dechloromonas* could be preferentially enriched for P-removal. Furthermore, Fujii et al. (2024) identified genes in *Zoogloea* associated with PHA accumulation, denitrification, sulfur metabolism and glycogen synthesis, suggesting its role in nutrient removal. Consequently, their co-existence enhances both the structural integrity and functional performance of the biofilm-based system. For SBR, spearman-based co-occurrence network, including samples before enrichment, shows four clusters based on modularity, where *Dechloromonas*, *Zoogloea*, *Accumulibacter*, *Propionivibrio*, and *Tessaracoccus* (as potential PAOs/GAOs) were clustered together. This cluster (dark-red coloured) exhibited mainly negative correlations with the cluster containing *Contendobacter* and *Competibacter*. It remains unclear whether the negative correlation between *Dechloromonas* and *Competibacter/Contendobacter* is due to direct competition or to the ability of these GAOs to occupy distinct ecological niches. Although the co-occurrence networks indicate a mutual influence of GAO presence, PAOs were dominant over GAOs at COD:P ratios under C-limiting conditions (adaptation V). This is in agreement with the study by Nielsen et al. (2019) showing that GAOs tend to be more abundant under surplus C-availability and that PAO-GAO competition is overestimated in the literature. When inoculum samples were excluded from the construction of network and nodes (representing genera) were ranked based on their betweenness centrality, *Dechloromonas* had a low betweenness centrality rank, suggesting weaker correlations with other genera, which contrasts with the pattern observed in the MMBS-relevant network (c.f. SI for spearman-based co-occurrence network, excluding samples before enrichment). This was not the case for *Competibacter*, *Contendobacter*, *Accumulibacter*, and *Zoogloea*, which showed higher ranks, emphasizing their greater dependency/influence within the network. In addition, the highly abundant bacterial family Saprospiraceae had a high betweenness centrality rank within the correlation network, suggesting that it correlated with multiple other genera and may play a central role in the community structure under the studied conditions. Its significant positive correlation with *Dechloromonas* and negative correlations with *Contendobacter* and *Competibacter* suggest its potential direct or indirect involvement in the observed P-removal efficiencies. As previously reported, members of the family Saprospiraceae have the potential to utilize polysaccharides, proteins, and other complex organics, perform partial nitrification, and store intracellular polymers such as glycogen and PHA (Kondrotaitė et al., 2022). The authors further confirmed that five different genera within this family could store glycogen or PHA, although poly-P accumulation was not observed.

4. Conclusions

The systematic analysis demonstrates that the C-source type exerts a more significant influence on the EBPR dynamics than the selected COD:P ratios, temperatures or pH values, supporting external C-dosing as a priority full-scale measure. Glucose was particularly effective in P-removal, while due to their limited efficiency ethanol and glycerol require anaerobic HRTs exceeding one hour, particularly as a potential strategy in WWTPs with flexible zone configurations. In biofilm-based system, biomass growth promotes P-uptake, but a high biofilm volume can restrict P-removal.

Dechloromonas plays a pivotal role in EBPR emphasizing its

previously underestimated contribution to the process, which still requires more targeted physiological and metabolic studies. PAOs have a growth advantage under carbon limitation and PAOs and GAOs can be mutually supportive. Accordingly, the competition between PAOs and GAOs does not exert a significant negative effect on P-removal performance. A clear correlation was observed between PAOs and bacteria of the Saprospiraceae family. We conclude that microbial diversity contributes to a reliable P-removal by enabling the dynamic enrichment of distinct genera under varying process conditions. In external dosing, diverse substrate composition can exploit the genera niche differentiation to enhance EBPR performance.

Declaration of Generative AI and AI-assisted technologies in the writing process

During the preparation of this work the authors used ChatGPT-4 (OpenAI) in order to improve the readability and language of this manuscript. After using this tool, the authors reviewed and edited the content as needed and take full responsibility for the content of the published article.

CRediT authorship contribution statement

Valerie Liese: Writing – review & editing, Writing – original draft, Visualization, Validation, Software, Methodology, Investigation, Formal analysis, Data curation, Conceptualization. **Berivan Akgün:** Writing – review & editing, Writing – original draft, Visualization, Validation, Methodology, Investigation, Formal analysis, Data curation, Conceptualization. **Ahmed Elreedy:** Writing – review & editing, Writing – original draft, Visualization, Validation, Software, Formal analysis, Data curation. **Jonas Lapp:** Writing – review & editing, Writing – original draft, Visualization, Validation, Supervision, Software, Methodology, Investigation, Formal analysis, Data curation, Conceptualization. **Kilian Ferle:** Software, Investigation. **Raphael Moll:** Validation, Resources. **Johannes Gescher:** Writing – review & editing, Writing – original draft, Validation, Supervision, Resources, Project administration, Methodology, Funding acquisition, Formal analysis, Conceptualization. **Tobias Morck:** Writing – review & editing, Writing – original draft, Validation, Supervision, Resources, Project administration, Methodology, Funding acquisition, Formal analysis, Conceptualization.

Declaration of competing interest

The authors declare the following financial interests/personal relationships which may be considered as potential competing interests: Valerie Liese reports financial support was provided by European Union. Valerie Liese reports financial support was provided by Federal state of Baden Württemberg, Germany. Berivan Akguen reports financial support was provided by Ministry of National Education of the Republic of Türkiye. If there are other authors, they declare that they have no known competing financial interests or personal relationships that could have appeared to influence the work reported in this paper.

Acknowledgement

The authors would like to thank the European Commission and the Ministry of Environment, Climate Protection and the Energy Sector of the federal state of Baden Württemberg, Germany, for funding the project *RoKKA* (Bioök_2076349). The second author (B. Akgün) acknowledges the Ministry of National Education of the Republic of Türkiye for providing a full doctoral scholarship to conduct this research. The authors thank the city of Erbach, Germany, and all involved persons of the wastewater treatment plants Erbach, Ulm-Steinhäule and Langenhagen for providing support and cooperation. The authors would furthermore like to thank deeply Dr. Ursula Telgmann, Dr. Julian Zinke, Andrea Brandl and Monika Degenhardt (University of

Kassel, Chair of Urban Water Engineering, Germany), as well as to Prof. Dr. Heidrun Steinmetz and Luciana Ninni Schaefer (RPTU Rheinland-Pfälzische Technische Universität Kaiserslautern-Landau, Department Resource Efficient Wastewater Technologies) for their excellent laboratory support, and to Edina Klein for her invaluable guidance and support throughout this research. The open-access publication was made possible thanks to financial support from the Open Access Publication Fund at Kassel University.

Appendix A. Supplementary data

Supplementary data to this article can be found online at <https://doi.org/10.1016/j.biortech.2025.133468>.

Data availability

Data will be made available on request.

References

- Aghilinasrollahabadi, K., Ghandehari, S., Kjellerup, B., Nguyen, C., Saavedra, Y., Li, G., 2024. Assessing the performance of polyphosphate accumulating organisms in a full-scale side-stream enhanced biological phosphorous removal. *Water Environ. Res* 96. <https://doi.org/10.1002/wer.10961>.
- An, W., Guo, F., Song, Y., Gao, N., Bai, S., Dai, J., Wei, H., Zhang, L., Yu, D., Xia, M., Yu, Y., Qi, M., Tian, C., Chen, H., Wu, Z., Zhang, T., Qiu, D., 2016. Comparative genomics analyses on EPS biosynthesis genes required for floc formation of *Zoogloea resiniphila* and other activated sludge bacteria. *Water Res.* 102, 494–504. <https://doi.org/10.1016/j.watres.2016.06.058>.
- Bauer, A., Wagner, M., Saravia, F., Bartl, S., Hilgenfeldt, V., Horn, H., 2019. In-situ monitoring and quantification of fouling development in membrane distillation by means of optical coherence tomography. *J. Membr. Sci.* 577, 145–152. <https://doi.org/10.1016/j.memsci.2019.02.006>.
- Bengtsson, S., 2009. The utilization of glycogen accumulating organisms for mixed culture production of polyhydroxyalkanoates. *Biotech Bioeng.* 104, 698–708. <https://doi.org/10.1002/bit.22444>.
- Broughton, A., Pratt, S., Shilton, A., 2008. Enhanced biological phosphorus removal for high-strength wastewater with a low rbCOD:P ratio. *Bioresour. Technol.* 99, 1236–1241. <https://doi.org/10.1016/j.biortech.2007.02.013>.
- Daims, H., 2009. Use of fluorescence in situ hybridization and the *daime* image analysis program for the cultivation-independent quantification of microorganisms in environmental and medical samples. *Cold Spring Harb. Protoc.* <https://doi.org/10.1101/pdb.prot5253>.
- Daims, H., Lückner, S., Wagner, M., 2006. *daime*, a novel image analysis program for microbial ecology and biofilm research. *Environ. Microbiol.* 8, 200–213. <https://doi.org/10.1111/j.1462-2920.2005.00880.x>.
- de Kreuk, M., van Loosdrecht, M., 2004. Selection of slow growing organisms as a means for improving aerobic granular sludge stability. *Water Sci. Technol.* 49, 9–17. <https://doi.org/10.2166/wst.2004.0792>.
- Dorofeev, A.G., Nikolaev, Y.A., Mardanov, A.V., Pimenov, N.V., 2020. Role of phosphate-accumulating bacteria in biological phosphorus removal from wastewater. *Appl. Biochem. Microbiol.* 56, 1–14. <https://doi.org/10.1134/S0003683820010056>.
- Egle, L., Rechberger, H., Krampe, J., Zessner, M., 2016. Phosphorus recovery from municipal wastewater: an integrated comparative technological, environmental and economic assessment of P recovery technologies. *Sci. Total Environ.* 571, 522–542. <https://doi.org/10.1016/j.scitotenv.2016.07.019>.
- Eichholz, C., Barjenbruch, M., Bannick, C.-G., Hartwig, P., 2023. A study on the situation and learnings of the precipitant shortage in the German wastewater sector. *Resources* 13, 1. <https://doi.org/10.3390/resources13010001>.
- Elahinik, A., Haarsma, M., Abbas, B., Pabst, M., Xevgenos, D., Van Loosdrecht, M.C.M., Pronk, M., 2022. Glycerol conversion by aerobic granular sludge. *Water Res.* 227, 119340. <https://doi.org/10.1016/j.watres.2022.119340>.
- Erdal, U.G., Erdal, Z.K., Daigger, G.T., Randall, C.W., 2008. Is it PAO-GAO competition or metabolic shift in EBPR system? Evidence from an experimental study. *Water Sci. Technol.* 58, 1329–1334. <https://doi.org/10.2166/wst.2008.734>.
- Filipe, C., Daigger, G., Grady, C., 2001. Effects of pH on the rates of aerobic metabolism of phosphate-accumulating and glycogen-accumulating organisms. *Water Environ. Res* 73, 213–222. <https://doi.org/10.2175/106143001X139191>.
- Fujii, N., Kuroda, K., Narihiro, T., Aoi, Y., Ozaki, N., Ohashi, A., Kindaichi, T., 2024. Unique epibiotic relationship between *Candidatus Patescibacteria* and *Zoogloea* in activated sludge flocs at a municipal wastewater treatment plant. *Environ. Microbiol. Rep.* 16, e70007. <https://doi.org/10.1111/1758-2229.70007>.
- Gonzalez-Garcia, R., McCubbin, T., Navone, L., Stowers, C., Nielsen, L., Marcellin, E., 2017. Microbial propionic acid production. *Fermentation* 3, 21. <https://doi.org/10.3390/fermentation3020021>.
- Guerrero, J., Tayà, C., Guisasola, A., Baeza, J., 2012. Glycerol as a sole carbon source for enhanced biological phosphorus removal. *Water Res.* 46, 2983–2991. <https://doi.org/10.1016/j.watres.2012.02.043>.
- Horn, M.A., Ihssen, J., Matthies, C., Schramm, A., Acker, G., Drake, H.L., 2005. *Dechloromonas denitrificans* sp. nov., *Flavobacterium denitrificans* sp. nov.,

- Paenibacillus anaericanus sp. nov. and Paenibacillus terrae strain MH72, N2O-producing bacteria isolated from the gut of the earthworm Aporrectodea caliginosa. *Int. J. Syst. Evol. Microbiol.* 55, 1255–1265. <https://doi.org/10.1099/ij.s.0.63484-0>.
- Kang, A.J., Munz, G., Yuan, Q., 2019. Influence of pH control on material characteristics, bacterial community composition and BNR performance of mature aerobic granules. *Process Saf. Environ. Prot.* 124, 158–166. <https://doi.org/10.1016/j.psep.2019.02.014>.
- Kim, J., Steinegger, M., 2024. Metabuli: sensitive and specific metagenomic classification via joint analysis of amino acid and DNA. *Nat. Methods* 21, 971–973. <https://doi.org/10.1038/s41592-024-02273-y>.
- Klein, E., Weiler, J., Wagner, M., Čeliković, M., Niemeyer, C.M., Horn, H., Gescher, J., 2022. Enrichment of phosphate-accumulating organisms (PAOs) in a microfluidic model biofilm system by mimicking a typical aerobic granular sludge feast/famine regime. *Appl. Microbiol. Biotechnol.* 106, 1313–1324. <https://doi.org/10.1007/s00253-022-11759-8>.
- Klein, E., Wurst, R., Rehlund, D., Gescher, J., 2024. Elucidating the development of cooperative anode-biofilm-structures. *Biofilm* 7, 100193. <https://doi.org/10.1016/j.biofilm.2024.100193>.
- Kolmogorov, M., Bickhart, D.M., Behsaz, B., Gurevich, A., Rayko, M., Shin, S.B., Kuhn, K., Yuan, J., Polevikov, E., Smith, T.P.L., Pevzner, P.A., 2020. metaFlye: scalable long-read metagenome assembly using repeat graphs. *Nat. Methods* 17, 1103–1110. <https://doi.org/10.1038/s41592-020-00971-x>.
- Kondrotaitė, Z., Valk, L.C., Petriglieri, F., Singleton, C., Nierychlo, M., Dueholm, M.K.D., Nielsen, P.H., 2022. Diversity and ecophysiology of the genus OLB8 and other abundant uncultured Saprospiraceae genera in global wastewater treatment systems. *Front. Microbiol.* 13, 917553. <https://doi.org/10.3389/fmicb.2022.917553>.
- Kutuzova, S., Piera, P., Nor Nielsen, K., Olsen, N.S., Riber, L., Gobbi, A., Forero-Junco, L. M., Dougherty, P.E., Westergaard, J.C., Christensen, S., Hansen, L.H., Nielsen, M., Nissen, J.N., Rasmussen, S., 2024. Binning meets taxonomy: TaxVAMB improves metagenome binning using bi-modal variational autoencoder. <https://doi.org/10.1101/2024.10.25.620172>.
- Laumeyer, C., Andrade Leal, M., Zimmer, J., de Best, J., Steinmetz, H., 2023. Technical report on pilot scale testing of PHA production and extraction from industrial residual streams. Project report, Wider Business Opportunities for Raw Materials from Wastewater-Capitalisation, Interreg North-West-Europe.
- Li, G., Srinivasan, V., Tooker, N.B., Wang, D., Yan, Y., Onnis-Hayden, A., Gu, A.Z., 2024. Distinct microdiversity of phosphate accumulating organisms (PAOs) between side-stream and conventional enhanced biological phosphorus removal (EBPR) systems with performance implications. *Water Res.* 266, 122280. <https://doi.org/10.1016/j.watres.2024.122280>.
- Li, H., 2016. Minimap and miniasm: fast mapping and de novo assembly for noisy long sequences. *Bioinformatics* 32, 2103–2110. <https://doi.org/10.1093/bioinformatics/btw152>.
- Liu, H., Zeng, W., Meng, Q., Fan, Z., Peng, Y., 2022. Phosphorus removal performance, intracellular metabolites and clade-level community structure of Tetrasphaera-dominated polyphosphate accumulating organisms at different temperatures. *Sci. Total Environ.* 842. <https://doi.org/10.1016/j.scitotenv.2022.156913>.
- Liu, R., Hao, X., Chen, Q., Li, J., 2019. Research advances of Tetrasphaera in enhanced biological phosphorus removal: a review. *Water Res.* 166, 115003. <https://doi.org/10.1016/j.watres.2019.115003>.
- Liu, Y., Chen, Y., Zhou, Q., 2007. Effect of initial pH control on enhanced biological phosphorus removal from wastewater containing acetic and propionic acids. *Chemosphere* 66, 123–129. <https://doi.org/10.1016/j.chemosphere.2006.05.004>.
- Liu, Y., Shi, H., Li, W., Hou, Y., He, M., 2011a. Inhibition of chemical dose in biological phosphorus and nitrogen removal in simultaneous chemical precipitation for phosphorus removal. *Bioresour. Technol.* 102, 4008–4012. <https://doi.org/10.1016/j.biortech.2010.11.107>.
- Liu, Z., Wang, Y., He, N., Huang, J., Zhu, K., Shao, W., Wang, H., Yuan, W., Li, Q., 2011b. Optimization of polyhydroxybutyrate (PHB) production by excess activated sludge and microbial community analysis. *J. Hazard. Mater.* 185, 8–16. <https://doi.org/10.1016/j.jhazmat.2010.08.003>.
- Loosdrecht, M.C.M., Nielsen, P.H., Lopez-Vazquez, C.M., Brdjanovic, D. (Eds.), 2016. *Experimental methods in wastewater treatment (chapter 2.2: Enhanced Biological Phosphorus Removal)*. IWA Publishing, London.
- Lopez-Vazquez, C., Hooijmans, C., Brdjanovic, D., Gijzen, H., van Loosdrecht, M., 2009. Temperature effects on glycogen accumulating organisms. *Water Res.* 43, 2852–2864. <https://doi.org/10.1016/j.watres.2009.03.038>.
- Lopez-Vazquez, C., Song, Y., Hooijmans, C., Brdjanovic, D., Moussa, M., Gijzen, H., van Loosdrecht, M., 2007. Short-term temperature effects on the anaerobic metabolism of glycogen accumulating organisms. *Biotechnol. Bioeng.* 97, 483–495. <https://doi.org/10.1002/bit.21302>.
- Majed, N., Gu, A., 2020. Phenotypic dynamics in polyphosphate and glycogen accumulating organisms in response to varying influent C/P ratios in EBPR systems. *Sci. Total Environ.* 743. <https://doi.org/10.1016/j.scitotenv.2020.140603>.
- Nguyen, P., Marques, R., Wang, H., Reis, M., Carvalho, G., Oehmen, A., 2023. The impact of pH on the anaerobic and aerobic metabolism of Tetrasphaera-enriched polyphosphate accumulating organisms. *Water Res.* X 19. <https://doi.org/10.1016/j.wroa.2023.100177>.
- Nielsen, P.H., Mclroy, S.J., Albertsen, M., Nierychlo, M., 2019. Re-evaluating the microbiology of the enhanced biological phosphorus removal process. *Curr. Opin. Biotechnol.* 57, 111–118. <https://doi.org/10.1016/j.copbio.2019.03.008>.
- Oehmen, A., Lemos, P., Carvalho, G., Yuan, Z., Keller, J., Blackall, L., Reis, M., 2007. Advances in enhanced biological phosphorus removal: from micro to macro scale. *Water Res.* 41, 2271–2300. <https://doi.org/10.1016/j.watres.2007.02.030>.
- Oehmen, A., Vives, M., Lu, H., Yuan, Z., Keller, J., 2005. The effect of pH on the competition between polyphosphate-accumulating organisms and glycogen-accumulating organisms. *Water Res.* 39, 3727–3737. <https://doi.org/10.1016/j.watres.2005.06.031>.
- Parks, D.H., Chuvochina, M., Rinke, C., Mussig, A.J., Chaumeil, P.-A., Hugenholtz, P., 2022. GTDB: an ongoing census of bacterial and archaeal diversity through a phylogenetically consistent, rank normalized and complete genome-based taxonomy. *Nucleic Acids Res.* 50, D785–D794. <https://doi.org/10.1093/nar/gkab776>.
- Puig, S., Coma, M., Monclús, H., van Loosdrecht, M., Colprim, J., Balaguer, M., 2008. Selection between alcohols and volatile fatty acids as external carbon sources for EBPR. *Water Res.* 42, 557–566. <https://doi.org/10.1016/j.watres.2007.07.050>.
- Sandeep, R., Muscolino, J.F., Macêdo, W.V., Piculell, M., Christenson, M., Poulsen, J.S., Nielsen, J.L., Vergeynst, L., 2023. Effect of biofilm thickness on the activity and community composition of phosphorus accumulating bacteria in a moving bed biofilm reactor. *Water Res.* 245, 120599. <https://doi.org/10.1016/j.watres.2023.120599>.
- Schindelin, J., Arganda-Carreras, I., Frise, E., Kaynig, V., Longair, M., Pietzsch, T., Preibisch, S., Rueden, C., Saalfeld, S., Schmid, B., Tinevez, J.-Y., White, D.J., Hartenstein, V., Elceiri, K., Tomancak, P., Cardona, A., 2012. Fiji: an open-source platform for biological-image analysis. *Nat. Methods* 9, 676–682. <https://doi.org/10.1038/nmeth.2019>.
- Shen, N., Zhou, Y., 2016. Enhanced biological phosphorus removal with different carbon sources. *Appl. Microbiol. Biotechnol.* 100, 4735–4745. <https://doi.org/10.1007/s00253-016-7518-4>.
- Singleton, C.M., Petriglieri, F., Kristensen, J.M., Kirkegaard, R.H., Michaelsen, T.Y., Albertsen, M.H., Kondrotaitė, Z., Karst, S.M., Dueholm, M.S., Nielsen, P.H., 2021. Connecting structure to function with the recovery of over 1000 high-quality metagenome-assembled genomes from activated sludge using long-read sequencing. *Nat. Commun.* 12, 2009. <https://doi.org/10.1038/s41467-021-22203-2>.
- Skenner, C.T., Barr, J.J., Slater, F.R., Bond, P.L., Tyson, G.W., 2015. Expanding our view of genomic diversity in *Candidatus* A cumuli bacter clades. *Environ. Microbiol.* 17, 1574–1585. <https://doi.org/10.1111/1462-2920.12582>.
- Smolders, G.J.F., Van Der Meij, J., Van Loosdrecht, M.C.M., Heijnen, J.J., 1994. Model of the anaerobic metabolism of the biological phosphorus removal process: Stoichiometry and pH influence. *Biotech Bioeng.* 43, 461–470. <https://doi.org/10.1002/bit.260430605>.
- Stokholm-Bjerregaard, M., Mclroy, S.J., Nierychlo, M., Karst, S.M., Albertsen, M., Nielsen, P.H., 2017. A critical Assessment of the Microorganisms Proposed to be Important to Enhanced Biological Phosphorus Removal in Full-Scale Wastewater Treatment Systems. *Front. Microbiol.* 8, 718. <https://doi.org/10.3389/fmicb.2017.00718>.
- Tian, X., Yin, X., Ji, X., Li, H., Duan, H., Zhang, K., Bian, D., 2025. The metabolic activity of phosphorus-accumulating organisms in response to low temperature in micro pressure swirl reactor. *J. Environ. Chem. Eng.* 13, 115036. <https://doi.org/10.1016/j.jece.2024.115036>.
- Wang, D., Zheng, W., Liao, D., Li, X., Yang, Q., Zeng, G., 2013. Effect of initial pH control on biological phosphorus removal induced by the aerobic/extended-idle regime. *Chemosphere* 90, 2279–2287. <https://doi.org/10.1016/j.chemosphere.2012.10.086>.
- Wang, F., Cui, Q., Liu, W., Ai, S., Liu, W., Bian, D., 2024. Synergistic denitrification mechanism of domesticated aerobic denitrifying bacteria in low-temperature municipal wastewater treatment. *npj Clean Water* 7, 6. <https://doi.org/10.1038/s41545-024-00299-5>.
- Winkler, M.-K.-H., Meunier, C., Henriot, O., Mahillon, J., Suárez-Ojeda, M.E., Del Moro, G., De Sanctis, M., Di Iaconi, C., Weissbrodt, D.G., 2018. An integrative review of granular sludge for the biological removal of nutrients and recalcitrant organic matter from wastewater. *Chem. Eng. J.* 336, 489–502. <https://doi.org/10.1016/j.cej.2017.12.026>.
- Zhao, C., Zhang, C., Shen, Z., Yang, Y., Qiu, Z., Li, C., Xue, B., Zhang, X., Yang, X., Wang, S., Wang, J., 2022. Ethylmalonyl-CoA pathway involved in polyhydroxyvalerate synthesis in *Candidatus* Contendobacter. *AMB Expr* 12, 39. <https://doi.org/10.1186/s13568-022-01380-3>.
- Zheng, J., Wang, N., Zhao, L., Li, Y., Yu, J., Wang, S., 2022. Microbial population changes and metabolic shift of *Candidatus* accumuli bacter under low temperature and limiting polyphosphate. *Water Sci. Technol.* 85, 1107–1119. <https://doi.org/10.2166/wst.2022.036>.
- Zheng, S., Bawazir, M., Dhall, A., Kim, H.-E., He, L., Heo, J., Hwang, G., 2021. Implication of surface properties, bacterial motility, and hydrodynamic conditions on bacterial surface sensing and their initial adhesion. *Front. Bioeng. Biotechnol.* 9, 643722. <https://doi.org/10.3389/fbioe.2021.643722>.